

Si(110)5×2-Au: A metallic chain structureJ. L. McChesney,* J. N. Crain,[†] and F. J. Himpsel*Department of Physics, University of Wisconsin Madison, 1150 University Avenue, Madison, Wisconsin 53706, USA*

R. Bennewitz

Department of Physics, McGill University, Montreal, Canada

(Received 5 April 2005; published 15 July 2005)

The Si(110) surface is found to form a stable 5×2 reconstruction upon incorporation of about eight gold atoms per (110)-5×2 unit cell. By means of scanning-tunneling microscopy we observe an array of one-dimensional chains with an internal double-row structure. Angle-resolved photoemission reveals that this reconstruction forms a metallic band which is split at the Fermi level.

DOI: [10.1103/PhysRevB.72.035446](https://doi.org/10.1103/PhysRevB.72.035446)

PACS number(s): 73.20.At, 79.60.Jv, 81.07.Vb, 68.37.Ef

INTRODUCTION

Electrons that are confined to lower dimensions exhibit a variety of exotic phenomena including the formation of charge density waves, spin density waves, and a divergence from breakdown of Fermi-liquid behavior. These properties stem from the fundamentally different physical properties that result in general from the confinement of electrons to lower dimensions, but also from the particular atomic realization of such a confinement. Probing the electronic structure helps to provide the understanding of physics governing these low-dimensional systems.

A variety of one-dimensional chain structures have been observed for Au on Si surfaces, making it a model system in which to investigate exotic electronic structures. By using Si(111) surfaces of varying vicinal miscut, the spacing between the Au-induced one-dimensional chains can be tuned and thus the interchain spacing. Crain *et al.*¹ demonstrated that the dimensionality of the resulting electronic system can be tailored through the interchain spacing. Smaller chain spacing leads to more dispersion perpendicular to the chains while at a large enough spacing there is no discernable interchain coupling within the resolution. In this report, we study the Au-induced reconstruction of the Si(110) surface, which in the systematic described above would be a Si(111) surface with a 35.3° miscut.

Though a low index plane, the clean Si(110) surface has a strong tendency towards faceting. Recent scanning-tunneling microscopy (STM) studies of the clean Si(110) surface reported details of the prevailing “16×2” surface reconstruction.² Röttger *et al.* also found some smaller areas which were reconstructed with a 5×1 periodicity.³ Such a 5×1 periodicity had been the subject of earlier STM studies.^{4,5} Some characteristic features of the atomic configuration from STM images of the 5×1 reconstruction are found again in the “16×2” reconstruction, indicating that the 5×1 periodicity is a favorite building block in this complex surface. It has actually been demonstrated that the 5×*n* reconstructions are stabilized by Ni impurities in the Si(110) surface.⁶

The deposition of Au on Si(110) effectively flattens and orders the Si(110) surface. Ino found a number of reconstruc-

tions for different coverage and annealing procedures.⁷ Out of these, the one-dimensional 2×5 reconstruction (which we will refer to as the 5×2 surface in order to compare with other studies of Au on silicon) is of particular interest for its similarity to the well studied Si(111)5×2-Au reconstruction.

The one-dimensional reconstruction of Si(110) upon submonolayer coverage of Au was exploited by Jalochowski *et al.* in a low-energy electron microscopy (LEEM) study of Pb nanowire formation.⁸ Following the results of Ino they pre-covered the Si(110) surface with a submonolayer of gold in order to obtain a flat surface with one-dimensional reconstruction, which indeed mediated the growth of elongated lead crystals through anisotropic diffusion and strain.

The aim of this work is to investigate the geometric structure of the Si(110)5×2-Au surface by means of STM, as well as the electronic structure by means of angle-resolved photoelectron emission, and to eventually establish a correlation between geometry and electronic structure in the framework of the previously studied Au induced reconstruction of vicinal Si(111) surface.

EXPERIMENT

The Si(110) surface was prepared following the same annealing sequence as used to prepare atomically straight single step arrays on Si(111).⁹ This heating sequence consists of outgassing the sample at 700 °C, flashing it to 1250 °C for less than 10 s, annealing it for 30 s at 1060 °C, annealing it for 120 s at 830 °C, and then quickly cooling it to room temperature. A precise coverage of Au is evaporated from a Mo filament bent into a basket. The evaporator is calibrated by reproducing the transition from the Si(111)5×2-Au to the Si(111) $\sqrt{3}\times\sqrt{3}$ -Au reconstruction which is observed by means of low-energy electron diffraction (LEED). This transition on the Si(111) surface occurs at a coverage of 0.4 monolayer (ML). The coverage refers to the Si(111) unit cell, where 1 ML corresponds to 15.66 nm⁻². The unit cell of the Si(110) surface has a size of 0.209 nm². Therefore, a scaling factor of 3.27 is used to calculate the number of gold atoms per (110) unit cell from the coverage calibrated to the Si(111) unit cell. Throughout this paper, the coverage is always given

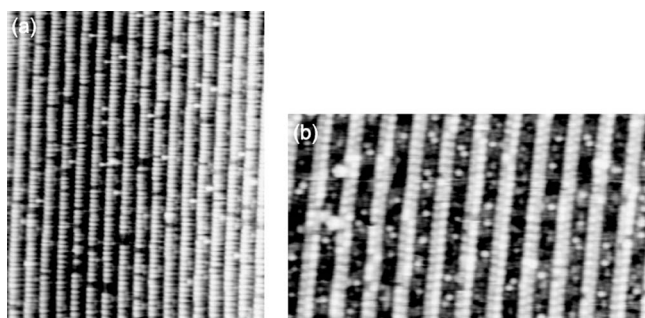


FIG. 1. Scanning tunneling microscopy images of the Si(110) 5×2 -Au surface. (a) Frame size $43 \times 52 \text{ nm}^2$, bias voltage -2 V , tunneling current 0.2 nA . (b) frame size $30 \times 17.5 \text{ nm}^2$, bias voltage $+2 \text{ V}$, tunneling current 0.2 nA .

in units of $ML_{(111)}$, i.e., monolayers with respect to the Si(111) unit cell.

The Si(110) 5×2 -Au surface is prepared by depositing a coverage of $0.26 ML_{(111)}$ Au onto the clean Si(110) surface which is held at $650 \text{ }^\circ\text{C}$. The coverage corresponds to 0.85 gold atoms per (110) unit cell. Prior to further measurements, the samples are annealed to $850 \text{ }^\circ\text{C}$ for a few seconds in order to remove any surface contaminants. The LEED pattern exhibits an $n \times 5$ periodicity across the chains and half-order streaks corresponding to a $n \times 2$ periodicity along the chains. We will show below that a 5×2 reconstruction is confirmed in scanning tunneling microscopy (STM) images.

Angle-resolved photoemission spectra have been recorded in order to reveal the dispersion of electronic bands at this surface reconstruction. The experiments have been performed at the Synchrotron Research Center using a Scienta 200 spectrometer with simultaneous energy and angle multidetection. The photoelectrons have been excited by p -polarized synchrotron radiation at a wavelength of $h\nu = 34 \text{ eV}$, exploiting a maximum in the cross section of Si surface states. During measurements the sample manipulator was kept a temperature of 10 K . The sample temperature is difficult to estimate. Analysis of the photoelectron emission at the Fermi edge from metal samples recorded with the same experimental setup suggests that the temperature is around $160\text{--}220 \text{ K}$.

RESULTS

Scanning-tunneling microscopy images of the Si(110) 5×2 -Au reconstruction reveal an array of one-dimensional chains (see Fig. 1). The chains run parallel to the $(-1 \ 1 \ 0)$ direction with an spacing of 2.7 nm , i.e., five times the length of 0.543 nm of the Si(110) unit cell. A high-resolution image is presented in Fig. 1(b). In this detail view, the chains appear to be composed of two close-by rows of protrusions, were one of the two rows sticks out farther than the other. Switch-over in contrast between the left and the right row occurs several times within one chain. This finding excludes tip artifacts as source for the double row appearance. The distance between protrusions along the chain is about 0.75 nm , close to twice the width of 0.384 nm of one Si(110)

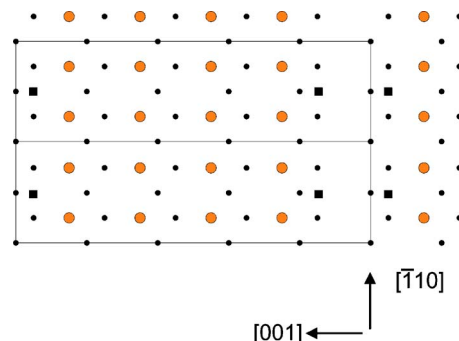


FIG. 2. (Color online) Schematic drawing of the Si(110) 5×2 -Au reconstruction. Small dots represent silicon atoms of the truncated bulk Si(110) surface. Large circles indicate the eight gold atoms incorporated per unit cell. Squares indicate the protrusions seen in the STM images. Note that the positions of gold atoms and protrusions with respect to the underlying Si lattice are uncertain at this point and have been included only to reflect the limited information obtained so far.

unit cell. The clear appearance of a double row versus a single row per unit cell is actually dependent on tunneling conditions. This is similar to the Si(111) 5×2 -Au reconstruction, where the appearance of atomic details of the structure in the STM images depends not only on the bias voltage, but also on the atomic constitution of the tip apex.¹⁰ Therefore, it is not possible to directly assign certain features in STM images either to protruding silicon atoms or to one of the eight gold atoms which are expected to be found in each 5×2 unit cell. In summary, our STM results clearly confirm the reconstruction in the form of a Si(110) 5×2 -Au surface, which is schematically drawn in Fig. 2.

The electronic structure of the Si(110) 5×2 -Au reconstruction was probed by mapping the energy band dispersions $E(k)$ along the chains. Figure 3 shows the photoelectron intensity as a function of energy and wave vector along the chains. Two bands can be clearly distinguished. The first band I is centered on the Γ point ($k_x=0 \text{ \AA}^{-1}$) and resembles an inverted parabola. The second band II is centered at the zone boundary of the $n \times 1$ unit cell and resembles a V shape which is split into two close subbands.

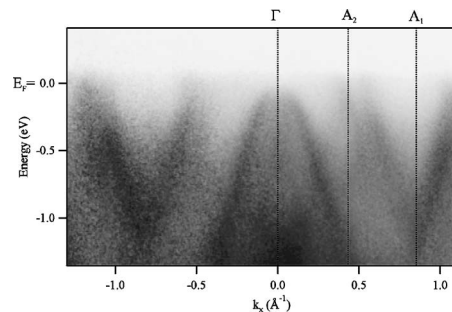


FIG. 3. Photoelectron intensity as a function of energy and wave vector along the chains on a Si(110) 5×2 -Au surface. Darker pixels indicate higher intensity. The zone boundary of the $n \times 2$ unit cell at 0.41 \AA^{-1} is labeled A_2 and the one of the $n \times 1$ unit cell at 0.82 \AA^{-1} is labeled A_1 . The inverted parabola in the center is named band I, the V-shaped features centered at A_1 are called band II.

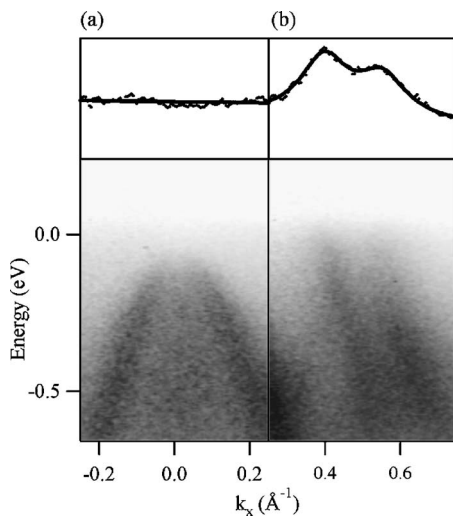


FIG. 4. Details of bands I and II (see Fig. 2) measured with longer integration time. The cross section in the upper part of the figure reveals the photoemission intensity at the Fermi energy. The solid lines represent fits to the data. Band I is fit to a linear background while the fits to band II are Lorentzian curves centered at 0.4 and 0.55 \AA^{-1} .

A measurement with longer integration time (Fig. 3) reveals details of bands I and II. The maximum of band I is found about 0.1 eV below the Fermi edge. This band might be a surface projection of the bulk valence band. It is interesting to note that no similar band has been found on any of the one-dimensional gold-induced reconstructions of vicinal Si(111) surfaces studied before.¹ Similar bands have been observed on the Si(111)- $\sqrt{3} \times \sqrt{3}$ -Au surface reconstruction¹¹ and for the Si(111)-3×1-Li surface reconstruction.¹²

Band II has clearly metallic character: Both branches of the split band II cross the Fermi level. The intensity at the Fermi level is drawn in the upper graph of Fig. 4. The symmetry with respect to the zone boundary point A1 indicates that band II has an $n \times 1$ periodicity, despite the $n \times 2$ appearance of the surface structure as revealed by STM. For the Si(110)-Au the Fermi edge crossing point is located at $k = 0.41 \text{\AA}^{-1}$ and $k = 0.55 \text{\AA}^{-1}$. The filling factors corresponding to these crossing points are 0.5 and 0.33, respectively.

DISCUSSION

The STM results demonstrate how effectively the rather instable Si(110) surface is stabilized through the Au-induced 5×2 reconstruction. The high-resolution images give some insight into the local structure, in particular the atomically straight chains of protrusions which emphasize the strong anisotropic character of this surface reconstruction. The chains are broken into segments of alternating contrast between the two rows of protrusions, and decorated with additional adatoms. Such characteristic features have been found for all Au induced reconstructions of vicinal Si(111) surfaces studied so far, i.e., Si(335)-Au, Si(557)-Au, Si(553)-Au, Si(775)-Au,¹ Si(111)5×2-Au,^{10,13} Si(111)337-Au,¹⁴ the facets of the Si(5512)-Au,¹⁵ and other miscuts.¹⁶ Electronic

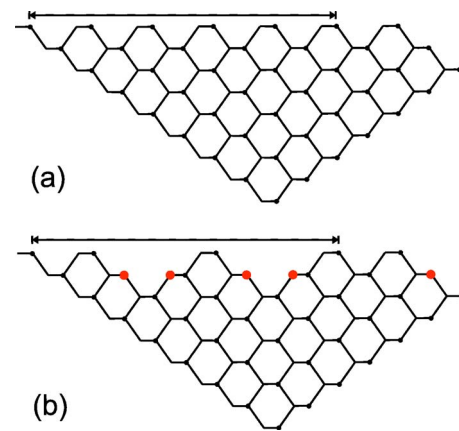


FIG. 5. (Color online) Schematic drawing of cuts perpendicular to the chains at the Si(110) surface [in the Si(1 -1 0) plane]. (a) The truncated bulk structure of Si(110), with the (110) surface at the top and two (111) facets at the bottom. (b) A tentative suggestion for the structure of Si(110)5×2-Au, based on the Au coverage and symmetry arguments.

structure calculations have shown that the chain features in STM images of the Si(111)5×2-Au surface cannot be attributed to Au atoms, but have to be assigned to the whole electronic structure.¹⁷ While we cannot draw any conclusions about the role of the atomic scale features for the stability of the Si(110)5×2-Au surface described here, it is worth mentioning that for the Si(111)5×2-Au the formation of metallic and semiconducting chain segments¹³ can be attributed to the electron doping effect of additional silicon adatoms.¹⁸ For chains forming on the Si(553)-Au surface it has been shown how the total energy of finite chain segments is lowered due to the existence of electronic end states.¹⁹ Considering the high miscut angle of the Si(110) surface with respect to the Si(111) surface it is surprising how closely the high-resolution STM images of the Si(110)5×2-Au reconstruction resemble those of Au-reconstructed Si(111) surface with lower miscut angle, in particular those of the Si(557)-Au surface.²⁰

Previous band structure measurements of Au induced chains on vicinal Si(111) surfaces have revealed metallic bands similar to the one reported here.^{21-23,1,18,14} In all cases, the bands are centered at the zone boundary and exhibit pronounced dispersion along the chain direction. The single split band for Si(110)-Au is particularly reminiscent of the similarly split band for the Si(557)-Au.²³ However, the splitting of the band of the Si(110)5×2-Au is significantly larger. The similarity with the results obtained on small-angle vicinal cuts of the Si(111) surface is somewhat surprising considering that these surfaces have unit cells that consist of single Si(111) terraces plus steps. It is not possible to determine the structure of the Si(110)5×2-Au surface from the STM data alone without a first-principles calculation. However, considering the similarities with the Si(557)-Au surface found in both the STM and the spectroscopy data, we draw a tentative picture of the structure in Fig. 5. Similar to the structure of the Si(557)-Au and other vicinal Si(111)-Au surfaces summarized in Ref. 1, the elementary building blocks are a gold chain incorporated into a Si(111) facet and steps.

If one scales the coverage of 0.26 monolayer by a factor of $\cos(35.3^\circ)$ for the projection onto a Si(111) facet the resulting coverage with respect to (111) facets is 0.21 monolayer, very close to the optimal Au coverage for the Si(557)-Au surface.

One can ask why the unusual splitting of a nearly half-filled band is a recurring phenomenon on Au-induced chain structures on silicon surfaces. The band splitting could be a combination of bonding and antibonding of two equivalent orbitals, such as two broken backbonds from Au to Si. A different approach independent of the structural details of each one-dimensional chain is to attribute the band splitting to spin-orbit coupling.²⁴ If the latter explanation holds for all Au induced metallic chain structures on silicon, the similarity of the splitting would be explained by a more basic physical phenomenon, while the differences in the rest of the elec-

tronic structure reflect the differences of the respective surface structures.

In summary, the Si(110) 5×2 -Au surface has been found to be a stable reconstruction with metallic character. Both high-resolution STM images and the electronic structure probed by angle-resolved photoemission exhibit strong similarities with Au-induced chain reconstruction of vicinal Si(111) surfaces with lower miscut angle.

ACKNOWLEDGMENTS

R.B. would like to acknowledge support from the University of Basel, Switzerland, in the initial phase of the project. The work was supported by the NSF under Grant No. DMR-0240937. It was conducted in part at the Synchrotron Radiation Center, which is supported by the NSF under Grant No. DMR-0084402.

*Present address: Department of Physics, Montana State University, Bozeman, Montana 59717.

†Present address: National Institute of Standards and Technology, Gaithersburg, Maryland 20899.

¹J. N. Crain, J. L. McChesney, Fan Zheng, M. C. Gallagher, P. C. Snijders, M. Bissen, C. Gundelach, S. C. Erwin, and F. J. Himpsel, *Phys. Rev. B* **69**, 125401 (2004).

²T. An, M. Yoshimura, I. Ono, and K. Ueda, *Phys. Rev. B* **61**, 3006 (2000).

³B. Röttger, M. Hanbücken, and H. Neddermeyer, *Appl. Surf. Sci.* **162–163**, 595 (2001).

⁴R. S. Becker, B. S. Swartzentruber, and J. S. Vickers, *J. Vac. Sci. Technol. A* **6**, 472 (1988).

⁵H. Neddermeyer and St. Tosch, *Phys. Rev. B* **38**, R5784 (1988).

⁶T. Ichinokawa, H. Ampo, S. Miura, and A. Tamura, *Phys. Rev. B* **31**, 5183 (1985).

⁷S. Ino, in *Reflection High-Energy Electron Diffraction and Reflection Electron Imaging of Surfaces*, Vol. 188 of *NATO Advanced Studies Institute, Series B: Physics*, edited by P. K. Larson and P. J. Dobson (Plenum Press, New York, 1988), p. 3.

⁸M. Jalochofski and E. Bauer, *Surf. Sci.* **480**, 109 (2001).

⁹J. L. Lin, D. Y. Petrovykh, J. Viernow, F. K. Men, D. J. Seo, and F. J. Himpsel, *J. Appl. Phys.* **84**, 255 (1998).

¹⁰A. Kirakosian, J. N. Crain, J. L. Lin, J. L. McChesney, D. Y. Petrovykh, F. J. Himpsel, and R. Bennewitz, *Surf. Sci.* **532**, 928 (2003).

¹¹K. N. Altmann, J. N. Crain, A. Kirakosian, J.-L. Lin, D. Y. Petrovykh, F. J. Himpsel, and R. Losio, *Phys. Rev. B* **64**, 035406

(2001).

¹²C. Bromberger, J. N. Crain, K. N. Altmann, J. J. Paggel, F. J. Himpsel, and D. Fick, *Phys. Rev. B* **68**, 075320 (2003).

¹³H. S. Yoon, S. J. Park, J. E. Lee, C. N. Whang, and I. W. Lyo, *Phys. Rev. Lett.* **92**, 096801 (2004).

¹⁴J. R. Ahn, H. W. Yeom, E. S. Cho, and C. Y. Park, *Phys. Rev. B* **69**, 233311 (2004).

¹⁵J. W. Dickinson, J. C. Moore, and A. A. Baski, *Surf. Sci.* **561**, 193 (2004).

¹⁶H. Okino, I. Matsuda, T. Tanikawa, and S. Hasegawa, *J. Surf. Sci. Nanotechnol.* **1**, 84 (2003).

¹⁷S. C. Erwin, *Phys. Rev. Lett.* **91**, 206101 (2003).

¹⁸J. L. McChesney, J. N. Crain, V. Perez-Dieste, Fan Zheng, M. C. Gallagher, M. Bissen, C. Gundelach, and F. J. Himpsel, *Phys. Rev. B* **70**, 195430 (2004).

¹⁹J. N. Crain and D. T. Pierce, *Science* **307**, 703 (2005).

²⁰R. Losio, K. N. Altmann, A. Kirakosian, J.-L. Lin, D. Y. Petrovykh, and F. J. Himpsel, *Phys. Rev. Lett.* **86**, 4632 (2001).

²¹P. Segovia, D. Purdie, M. Hengsberger, and Y. Baer, *Nature (London)* **402**, 504 (1999).

²²F. J. Himpsel, K. N. Altmann, R. Bennewitz, J. N. Crain, A. Kirakosian, J.-L. Lin, and J. L. McChesney, *J. Phys.: Condens. Matter* **13**, 11097 (2001).

²³J. N. Crain, A. Kirakosian, K. N. Altmann, C. Bromberger, S. C. Erwin, J. L. McChesney, J.-L. Lin, and F. J. Himpsel, *Phys. Rev. Lett.* **90**, 176805 (2003).

²⁴D. Sánchez-Portal, S. Riikonen, and R. M. Martin, *Phys. Rev. Lett.* **93**, 146803 (2004).